Power spectrum of small-scale turbulent velocity fluctuations in the solar wind

J. J. Podesta,[1] D. A. Roberts,[1] and M. L. Goldstein[1]

[1]   It is well known that the power spectrum of magnetic field fluctuations in the solar wind exhibits a Kolmogorov spectrum $f^{-\alpha}$ in the inertial range of the turbulence with a power law exponent α near 5/3. The power spectrum of velocity fluctuations has not been as well studied, partly because of the lack of high time resolution measurements needed to resolve a significant fraction of the inertial range. In situ measurements in the ecliptic plane at 1 AU acquired by the 3DP instrument on board the Wind spacecraft near solar minimum in 1995 are used to determine power spectra of the proton bulk velocity fluctuations between 10^{-5} and 10^{-1} Hz. The spectrum for the proton kinetic energy (the sum of the spectra for the individual components V_x, V_y, and V_z) obtained using 3-s velocity data is found to possess the spectral exponent $\alpha = 1.50$ in the inertial range of the turbulence. A similar calculation of the magnetic energy spectrum yields the exponent $\alpha = 1.67$. The Alfvén ratio, the ratio of the kinetic to magnetic energy spectrum, is a slowly increasing function of frequency throughout the inertial range increasing from approximately 0.5 to 1 in the frequency interval from 10^{-4} to 10^{-2} Hz. This indicates that the partition of energy between small-scale velocity and magnetic field fluctuations is frequency-dependent, contrary to some theories. The total energy spectrum (kinetic plus magnetic) has the power law exponent 3/2. A brief investigation of high- and low-speed solar wind streams is also performed, which shows that different spectral exponents for velocity and magnetic field fluctuations are observed in both high- and low-speed wind.

1.   Introduction

[2]   Recent studies of solar wind power spectra [*Podesta and Roberts*, 2005; J. Borovsky, The velocity fluctuations of the solar-wind turbulence as compared with the magnetic-field fluctuations: Spectral indices, turbulence amplitudes, and solar-wind discontinuities, submitted to *Journal of Geophysical Research*, 2006] and structure functions [*Salem*, 2000; *Mangeney et al.*, 2001] suggest that turbulent velocity fluctuations in the solar wind are characterized by a power law spectrum $f^{-\alpha}$ in the inertial range where f is the frequency in Hertz and the exponent α has a value near 1.5. The value of the power law exponent for the velocity fluctuations is therefore different from the power law exponent for the magnetic field fluctuations $\alpha \simeq 1.67$ [*Goldstein et al.*, 1995; *Leamon et al.*, 1998; *Goldstein and Roberts*, 1999]. The differences between the spectral indices of velocity and magnetic field fluctuations is an important observation which raises some interesting theoretical questions. A more precise knowledge of these spectral exponents is important for improving our understanding of MHD turbulence and the relationship between velocity and magnetic field fluctuations in the solar wind.

[3]   The purpose of this study is to use in situ solar wind measurements to obtain improved estimates of the power law exponent for turbulent velocity fluctuations in the solar wind. These estimates are difficult to perform because the sampling rate of existing measurements of the bulk proton velocity are usually not high enough to resolve a significant fraction of the inertial range. As a consequence, estimates of the power law exponent α are corrupted by aliasing errors. Measurements with higher sampling rates are needed to explore the upper end of the inertial range.

[4]   The 3DP instrument on board the Wind spacecraft [*Lin et al.*, 1995] has a nominal 3 s sampling rate, the fastest data rate available from any solar wind plasma instrument now in service. The 3DP data that is processed on the ground, called PLSP data (Pesa Low Energy Spectra), is more carefully calibrated and has a nominal 24 s sampling rate. During the first year of its mission there are a few time periods where PLSP data with sampling rates of approximately 12.5 s are available. One such time period early in the mission is shown in Figure 1.

[5]   As one can see from the top panel in Figure 1, the data for this 7 day interval cannot be considered approximately stationary and therefore it is not suitable for power spectral analysis. Because the trend is nonlinear, any attempt at trend removal is risky and may alter the spectrum in unacceptable

---

[1]Laboratory for Solar and Space Physics, NASA Goddard Space Flight Center, Greenbelt, Maryland, USA.
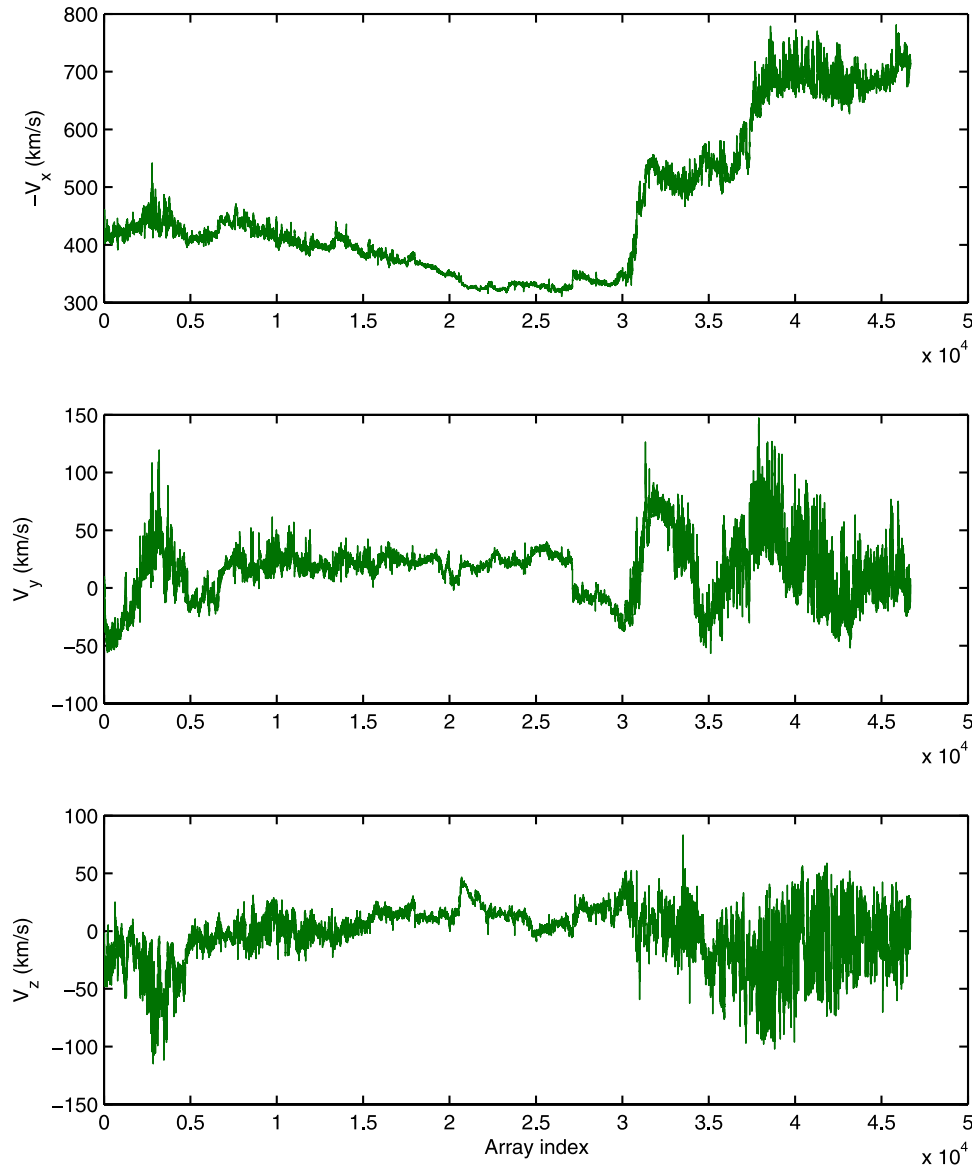
Figure 1. Proton velocity data (3DP PLSP data) for the time period 28 December 1994 1830:39 through 4 January 1995 1735:38. The data for this particular time interval are sampled at a rate of approximately 12.8 s with a few small data gaps.

ways. For the purposes of spectral analysis the most prudent approach is to identify subintervals where the average velocity is approximately constant or contains a linear trend and to analyze these intervals separately.

[6] However, with this approach different spectral slopes are generally found for the different subintervals and there is no unique answer to the question: what is the spectral exponent? The problem is that the record length is too short to permit a unique determination of the spectral exponent. A possible solution is to choose a record which is devoid of trends and long enough to sample the complete range of solar wind conditions in their normal proportions including fast and slow speed streams, shocks, and quiet periods. To satisfy these requirements, the record length must be much greater than a solar rotation period, at least five or ten Bartels rotations. Because the nature of solar wind turbu-

lence is known to vary with the solar cycle, it is also desirable to choose the record length much less than 11 years (or 22 years if one includes the magnetic polarity of the cycle). This allows one to investigate the possibility of different spectral exponents at different points in the solar cycle. One may also consider a ''solar cycle averaged spectral exponent'' obtained from data records much longer than one solar cycle.

[7] Optimally, one would like a data record from 1 to 3 years in duration with a uniform sampling time of 3 s or less. To fully resolve the transition from the inertial range to the dissipation range of the turbulence would require a much faster sampling rate on the order of 10 Hz. Such sampling rates are unavailable for plasma velocity, although they are now abundant for the magnetic field.

[8] The competing requirements of high sampling rate and long continuous record length can be met using the 3-s onboard plasma moments from the Wind 3DP instrument. This data is sometimes noisy since it is computed on board the spacecraft but continuous measurements are available for the entire mission except for occasional data gaps. To ascertain whether this 3-s data can be used to obtain reliable power spectra, it is possible to compare the 3-s spectra with spectra computed from 24-s 3DP data and the occasional 12.5-s 3DP data. The 24 and 12.5 s data is processed on the ground by the 3DP instrument team at Berkeley Space Science Laboratory and is more reliable than the 3-s data. This is the approach adopted here.

[9] The integrity of velocity power spectra based on 3-s 3DP data is established by first using small time intervals on the order of one day. The size of the time intervals employed in the analysis is then gradually increased until the desired record size is reached, typically several Bartels rotations. Comparison against power spectra obtained using more accurate 24-s 3DP data is performed at each stage for purposes of quality control. A brief outline of this paper is as follows. Section 2 presents a comparison between spectra obtained from the high- and low-resolution data. Estimates of aliasing errors are computed in section 3. Power spectra and spectral exponents for a time interval spanning two Bartels rotations are presented in section 4. The Alfvén ratio is examined in section 5. Spectral exponents for fast and slow speed wind are discussed in section 6. The conclusions are summarized in section 7.

2. Comparison Between 3-s Data and 12.8-s Data

[10] The 3-s 3DP plasma moments computed on-board the spacecraft are noisier and less dependable than the carefully prepared 24-s 3DP data product (PLSP data) which is processed on the ground. The 3-s velocity measurements are reasonably accurate, however, as can be seen by comparing plots of the 3-s velocity data to the 24-s data. In this section proton velocity spectra computed from the 3-s data are compared to power spectra computed from the more carefully processed 24-s data. Such comparisons suggest that 3-s data is suitable for the calculation of velocity power spectra. Moreover, they illustrate the severe limitations of aliasing errors for the estimation of spectral exponents as will be shown in this section.

[11] The first interval studied is the high speed solar wind stream seen on the right-hand side of Figure 1. The high speed stream extends from approximately 3.8×10^4 to 4.7×10^4 in Figure 1 or, more precisely, from 3 January 1995 1255:39 to 4 January 1995 1735:38 (hereafter, time interval 1). Within this interval the three velocity components undergo fluctuations about the mean value, but there are no obvious trends which would indicate nonstationarity of the time series in this interval.

[12] Before power spectra can be computed, the data is arranged into an approximately uniformly sampled time series and the data gaps are linearly interpolated. The sampling time (the time interval between measurements) varies due to small changes in the spin rate of the spacecraft. For the 1.2 day subinterval under consideration, interval 1, the average sampling time omitting gaps is $t_s = 12.7944$ s

with a standard deviation of 8.0×10^{-3} s. There are 11 data gaps which range in size from $4t_s$ to $13t_s$. The duration of all data gaps are found to be an integer multiple of the average sampling time, to a high degree of approximation. Therefore it is reasonable to arrange the data into a "uniformly sampled" time series with a sampling time of 12.7944 s. The same technique is applied to the 3-s data which for time interval 1 has an average sampling time, omitting gaps, of $t_s = 3.1987$ s. In addition, for the 3-s data there are 11 data gaps ranging in size from $17t_s$ to $49t_s$.

[13] Power spectra are computed by means of a smoothed periodogram. First, the mean is subtracted from the data, then the length of the data record is doubled by zero padding, the FFT is applied, and the resulting periodogram is smoothed by convolution with a Papoulis smoothing window as described, for example, in chapter 6 of *Percival and Walden* [1993]. This is referred to as a lag window spectral estimator with a Papoulis lag window. Due to the large dynamic range in turbulence spectra the smoothing is performed with a frequency dependent bandwidth Δf given by $\Delta f = af$ where $a = 0.3$. No data tapering is used because, due to the large sample size, the bias error without tapering is expected to be small. Moreover, the bias error is approximately independent of frequency in the inertial range [*Podesta*, 2006] so that it does not distort the spectral estimate. Note that all frequency spectra presented below are measured with respect to the reference frame of the spacecraft.

[14] The power spectra for the components V_x, V_y, and V_z are shown in Figure 2. Inspection of Figure 2 indicates that the power spectra obtained from both the 3-s 3DP data and the 12.8-s data are in agreement until aliasing errors in the power spectrum for the 12.8-s data become noticeable, that is, for frequencies greater than approximately 4×10^{-3} Hz. The main conclusion to be drawn from this and the following Figure is that the 3-s data can indeed be used to obtain accurate power spectra for the proton velocity.

[15] The spectrum for total kinetic energy, the sum of the individual power spectra for V_x, V_y, and V_z (GSE components) is shown in Figure 3. The use of 3-s data versus 24-s data allows the inertial range spectrum to be extended by almost a full decade in frequency space. This is significant for studies of the spectral exponents.

[16] The aliasing errors in Figures 2 and 3 arise whenever a continuous time signal is sampled in discrete time. In general, for a spectrum with a power law decay the aliasing errors are large not only in the neighborhood of the Nyquist frequency but throughout much of the preceding decade in frequency space. This fact, discussed more thoroughly in the next section, has important implications for the estimation of spectral exponents. For example, even though the aliasing error for V_x at 1×10^{-2} Hz looks small to the eye in Figure 2, top, least squares fits to the power spectra for data between 1×10^{-3} and 1×10^{-2} Hz yield the power law exponents -1.41 for the 3-s data and -1.32 for the 12.8-s data. The large discrepancy between these two values is due to aliasing errors in the spectrum for the 12.8-s data. Because aliasing cannot be eliminated, this example shows that it is important to restrict estimates of spectral exponents to regions where the aliasing errors are negligible.

[17] For completeness it should be mentioned that least squares fits to the power spectra for V_y, V_z, and the total
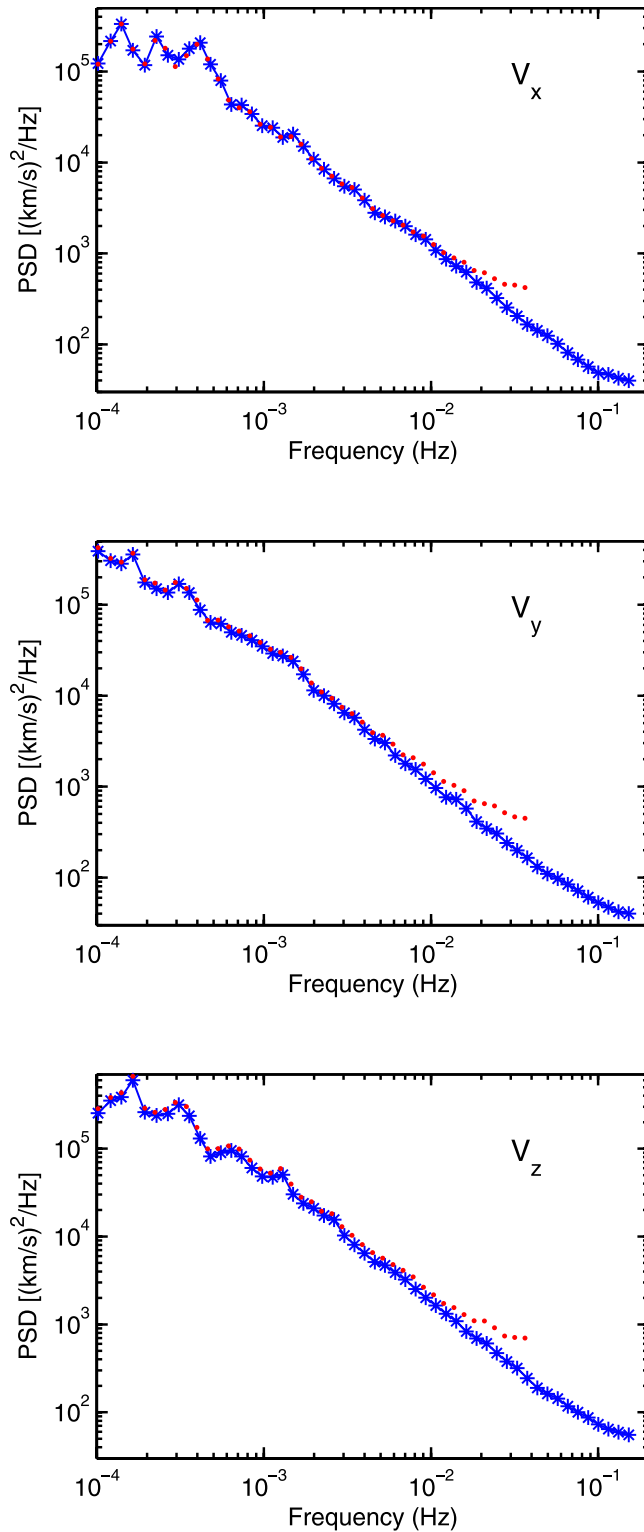
Figure 2. Power spectra for the proton velocity components in GSE coordinates computed from the 3-s 3DP data (blue stars) and 12.8 s PLSP data (red dots) for the time period 3 January 1995 1255:39 to 4 January 1995 1735:38.

kinetic energy between 1×10^{-3} and 1×10^{-2} Hz yield the power law exponents -1.56, -1.53, and -1.51 for the 3-s data, respectively, and -1.46, -1.47, and -1.45 for the 12.8-s data, respectively. The large differences between the

exponents obtained from the 3-s data and 12.8-s data are primarily due to aliasing errors in the spectra for the 12.8-s data.

3. Analysis of Aliasing Errors

[18] In practice, it is important to know the magnitude of aliasing errors so that aliasing effects can be avoided or minimized when estimating spectral exponents. These errors are easy to estimate for spectra with a power law decay such as those encountered in solar wind turbulence. The power spectrum of velocity fluctuations can be approximated by the simple function

$$S(f) = \frac{S_0}{1 + |f/f_0|^{\alpha}}, \tag{1}$$

where S_0 is constant and the frequency f_0 marks the beginning of the power law decay of the spectrum. Only the frequency range $f \gg f_0$ is of interest here (the dissipation range is not included in the model spectrum because it occurs at much higher frequencies than any of the frequencies measured).

[19] When the velocity signal is sampled at evenly spaced time intervals Δt, the power spectrum of the sampled signal is given by

$$S_a(f) = \sum_{n=-\infty}^{\infty} S(f - nf_s), \tag{2}$$

where $f_s = 1/\Delta t$ is the sampling frequency and $S(f)$ is the power spectrum before sampling given by equation (1). Here $|f| \leq f_{NQ}$ where $f_{NQ} = 1/(2\Delta t)$ is the Nyquist frequency. Equation (2) shows that the power spectrum of
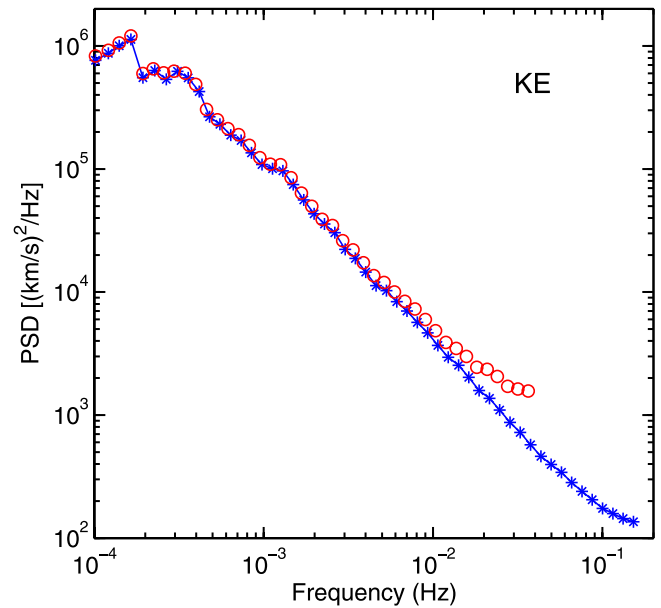
Figure 3. Power spectrum for the total kinetic energy computed from 3-second 3DP data (blue stars) and 12.8 s PLSP data (red circles) for the time period 3 January 1995 1255:39 to 4 January 1995 1735:38.
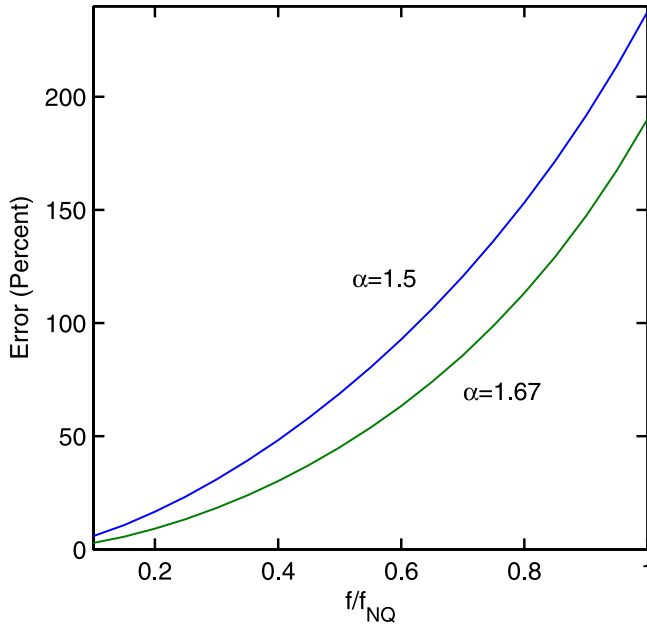
Figure 4. Aliasing error E versus frequency for power spectra with exponents $\alpha = 1.5$ and 1.67. At the frequency $f = f_{NQ}/10$ the errors are 5.8 and 2.9 percent for the exponents $\alpha = 1.5$ and 1.67, respectively.

the sampled signal contains power from all the higher harmonics $n \neq 0$. This is the source of aliasing.

[20] The spectrum $S_a(f)$ is the power spectrum which is estimated from the measured data. The error between the measured (aliased) spectrum $S_a(f)$ and the spectrum of the underlying process $S(f)$ is given by

$$E(f) = \frac{S_a(f) - S(f)}{S(f)}, \qquad (3)$$

where $|f| \leq f_{NQ}$. Inserting equation (2), one may write the previous equation in the form

$$E(f) = E_+(f) + E_-(f), \qquad (4)$$

where

$$E_\pm(f) = \frac{\sum_{n=1}^{\infty} S(f \pm nf_s)}{S(f)}. \qquad (5)$$

It is convenient to let $x = f/f_{NQ}$ so that the frequency is expressed in Nyquist units. It will be shown that the aliasing error is only significant when $0.1 < x < 1$. This inequality is assumed to hold in what follows. For solar wind spectra that possess a power law decay spanning several decades in frequency the condition $f_0 \ll f_{NQ}$ is well satisfied. Substituting the power spectrum (1) into equation (5) and using the previous inequalities, one obtains the approximation

$$E_\pm(x) \simeq \sum_{n=1}^{\infty} \frac{x^\alpha}{(2n \pm x)^\alpha}, \qquad (6)$$

where $0.1 < x < 1$. This sum is evaluated numerically for different values of $\alpha > 1$ to obtain the error curves shown in Figure 4. The error estimates show that the aliasing errors are monotonically increasing and remain significant throughout most of the interval $0.1 < x < 1$. Therefore for the spectra studied in this paper it is recommended that this interval be omitted when computing spectral exponents. This practice is followed throughout.

4. Power Spectrum of a 54-Day Interval

[21] The largest time interval analyzed in this study is a 54-day interval (2 Bartels rotations) around solar minimum between 23 May 1995 0000:00 and 16 July 1995 0000:00. The velocity data for this interval are shown in Figure 5. Two successive high speed streams occur near the beginning of this interval, the first located near day of year 145 and the second near day 152. The first stream strengthens and is seen again during the next Bartels rotation around day 172. The second stream weakens considerably and appears to split into two streams on the next Bartels rotation as seen around days 178 and 182. Between these high-speed streams are found periods of very low speed wind. As can be seen in Figure 5 there do not appear to be any obvious trends in the data that would adversely affect the estimation of power spectra.

[22] For this particular time interval the time steps Δt between measurements ranges from 2.52 s to 7535 s or 2.09 hours. Between 2.5 and 3.6 s the distribution of time steps is tightly clustered about the mean value 3.01858 s. Time intervals greater than 3.6 s are called data gaps. Data gaps range in size from 6 s to 2.09 hours. There are three data gaps approximately 2 hours in length, nine data gaps with lengths between 7 min and 1.2 hours, and many smaller data gaps. The are 576 data gaps in all with a sum total duration of 1.00 days. The total duration of the data gaps account for 1.85 percent of the total record length.

[23] To construct a "uniformly spaced" time series, each time step Δt, including the data gaps, is rounded to the nearest integer multiple of 3.01858 s. The data gaps are then linearly interpolated to produce a time series of length $N = 1545628$ which is ready for spectral analysis using Fourier FFT techniques. Because the data gaps represent a small percentage of the data, the interpolation of the data gaps is not expected to have a significant effect on the power spectral estimates. The mean value of (V_x, V_y, V_z) for the interpolated time series is given by $(-435.45, 13.51, -5.15)$ km/s.

[24] The power spectrum for the kinetic energy, the sum of the individual power spectra for V_x, V_y, and V_z, is shown in Figure 6. The bandwidth of the smoothing window used to smooth the spectra of the velocity components is given by $\Delta f = f/10$. The slope of the spectrum is roughly constant from 1×10^{-4} Hz up to the Nyquist frequency 1.66×10^{-1} Hz. To estimate the spectral exponent a linear least squares fit was performed for the data in the subinterval $1 \times 10^{-3} \leq f \leq 1 \times 10^{-2}$ Hz. The spectral exponent is found to be -1.50. The end point of the interval 1×10^{-2} Hz is more than a decade less than the Nyquist frequency so the estimate of the spectral exponent is not contaminated by aliasing errors. If the upper limit of the subinterval is changed to 2×10^{-2} Hz, then the spectral exponent changes to -1.49.
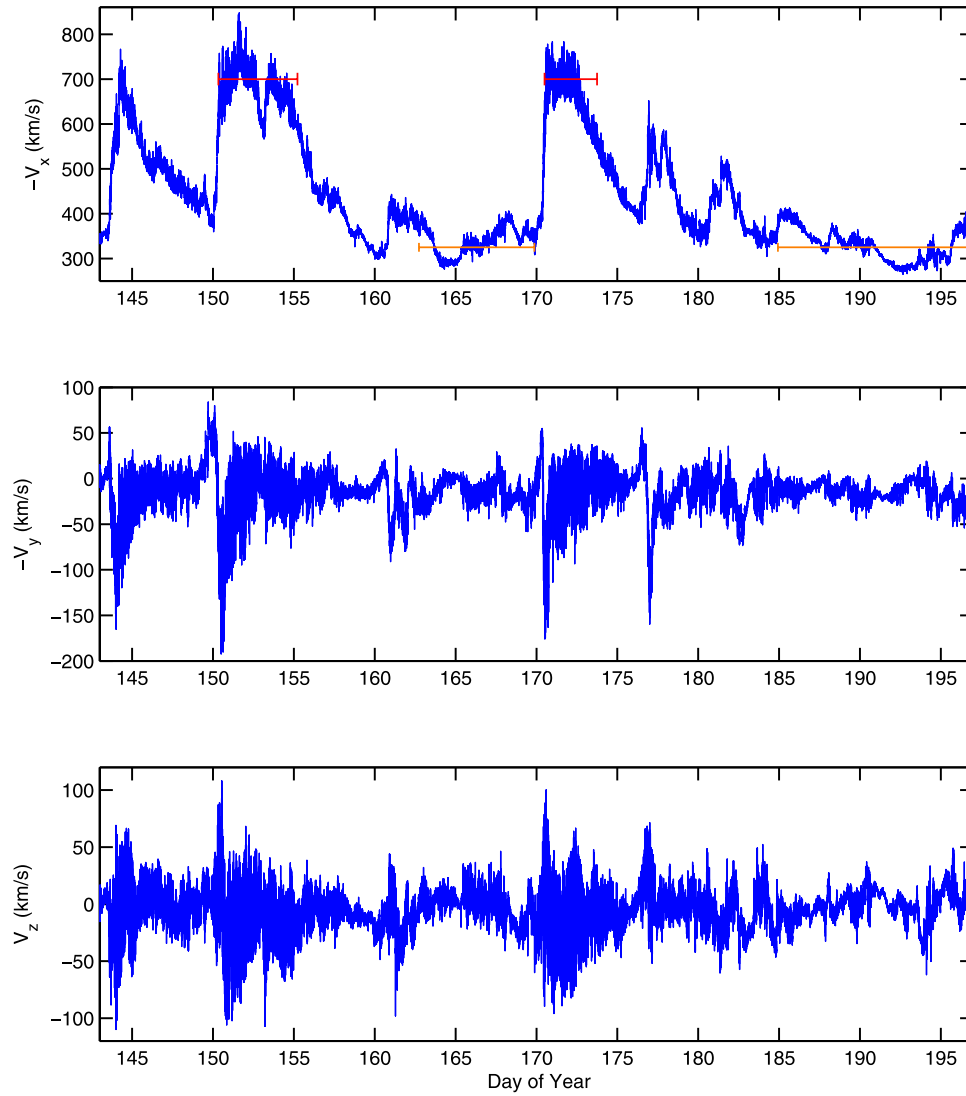
Figure 5. Proton velocity data for the time period 23 May 1995 00:00:00 through 16 July 1995 0000:00. The subintervals containing high and low speed wind are indicated by the red and orange markers, respectively.

If the lower limit of the subinterval is changed to 5×10^{-4} Hz, then the spectral exponent changes to -1.47. Therefore the estimate -1.50 is not sensitive to the exact location of the endpoints of the subinterval.

[25] For purposes of comparison, the power spectrum of the magnetic energy, equal to the sum of the power spectra for the components B_x, B_y, and B_z, is shown in Figure 6, bottom. The magnetic spectra were computed using 3-s averages of the magnetic field vector obtained by the Wind MFI instrument [*Lepping et al.*, 1995]. The spectral exponent found for the magnetic spectrum in the subinterval $1 \times 10^{-3} \leq f \leq 1 \times 10^{-2}$ Hz is found to be -1.66, consistent with the studies of *Leamon et al.* [1998] and others. If the upper limit of the subinterval is changed to 2×10^{-2} Hz, then the spectral exponent is unchanged. If the upper limit of the subinterval is changed to 2×10^{-2} Hz and the lower limit of the subinterval is changed to 5×10^{-4} Hz, then the spectral exponent changes to -1.64. Therefore the estimate -1.66 is

not sensitive to the exact location of the endpoints of the subinterval.

[26] A subtle difference between the kinetic and magnetic spectra shown in Figure 6 is what appears to be a lack of aliasing in the magnetic spectrum. This is due to the fact that the 11 Hz sampling rate of the MFI instrument is much greater than the Nyquist frequency 0.1667 Hz of the power spectrum in Figure 6 (bottom) so that after averaging the MFI data in 3-second intervals the aliasing errors in Figure 6 (bottom) are negligible. Thus the spectral exponents estimated from the magnetic field data can be extended to higher frequencies. For the subinterval $1 \times 10^{-3} \leq f \leq 5 \times 10^{-2}$ Hz the spectral exponent is found to be -1.67.

[27] Because the error in the spectral exponents is typically on the order of 2 or 3 percent, one may conclude that the kinetic and magnetic energy spectra have significantly different power law exponents in the inertial range of the turbulence. A clear demonstration of this fact based on
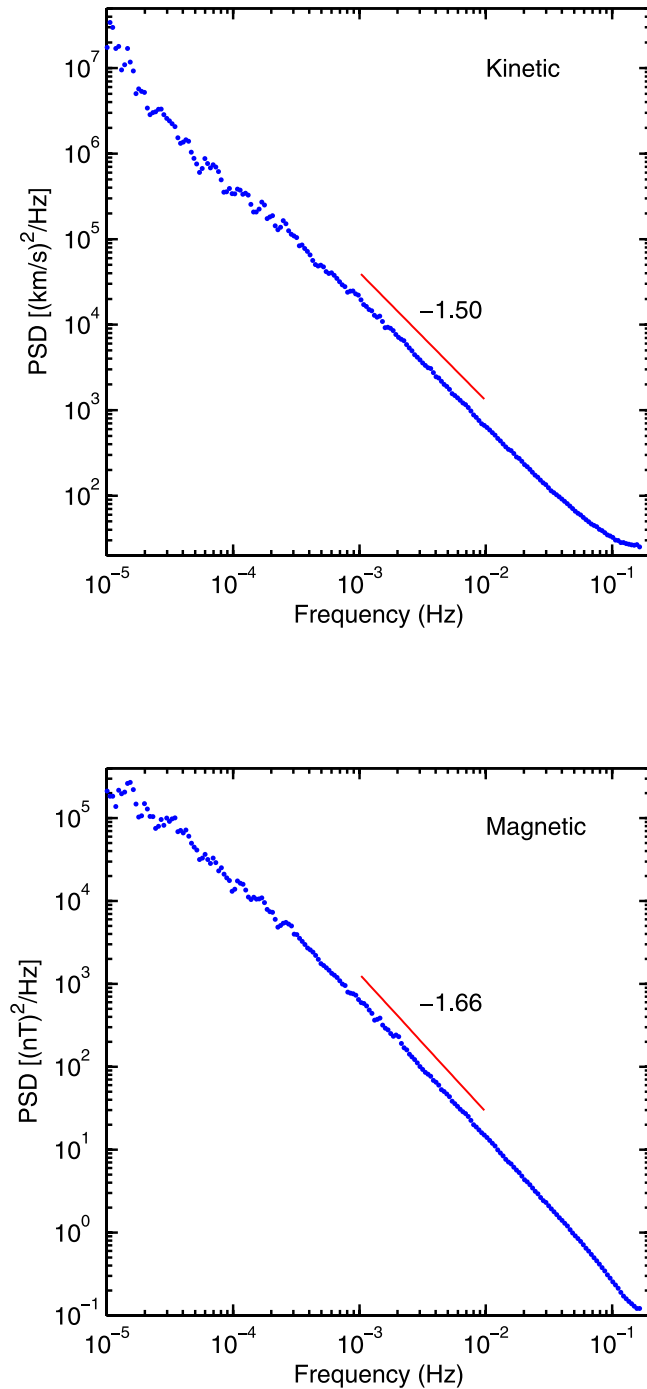
Figure 6. Power spectra for the total kinetic energy (top) computed from 3-s 3DP data for the 54 day period 23 May 1995 0000:00 through 16 July 1995 0000:00. Power spectra for the total magnetic energy (bottom) computed from 3-s MFI data for the same 54 day period. The best fit straight line over the interval $1 \times 10^{-3} \leq f \leq 1 \times 10^{-2}$ Hz is indicated by the red line segment.

the magnetic field components B_x, B_y, and B_z are -1.67, -1.63, and -1.68, respectively.

5. Alfvén Ratio

[28] It is of interest to compare the relative magnitudes of kinetic and magnetic power spectra. However, to do this the density fluctuations must be incorporated into either the velocity or magnetic field variables before performing the spectral analysis so that the resulting kinetic and magnetic energy spectra have the same dimensions. This is left for future research. For now, a rough comparison is performed by converting the magnetic field to velocity units $B/(\mu_0\rho)^{1/2}$ where μ_0 is the permeability of free space, $\rho = 1.17\ m_p n_p$ is the average mass density of the solar wind, m_p is the proton mass, $n_p = 9.4$ cm^{-3} is the average proton density at 1 AU during the 54 day interval, and the factor 1.17 accounts for the contribution to the solar wind mass density from alpha particles assuming $n_p/n_\alpha = 24$. This yields the Alfven ratio, the ratio of kinetic to magnetic energy spectra, shown in Figure 7.

[29] The sharp rise in the Alfven ratio beyond 1×10^{-2} or 2×10^{-2} Hz in Figure 7 is not a real effect but is caused by aliasing in the velocity spectrum. The average Alfvén ratio between 1×10^{-3} and 1×10^{-2} Hz is 0.87 indicating the rough equipartition, in the first order of approximation, between the velocity and magnetic field fluctuations. However, because the magnetic energy spectrum decreases faster than the kinetic energy spectrum the Alfvén ratio increases slightly throughout the inertial range. This implies that the partition of energy between small scale velocity and magnetic field fluctuations is not in a constant ratio in the inertial range. The observed increase in the Alfvén ratio is not large due to the small difference in the spectral exponents of v and B but is certainly measurable as shown here.
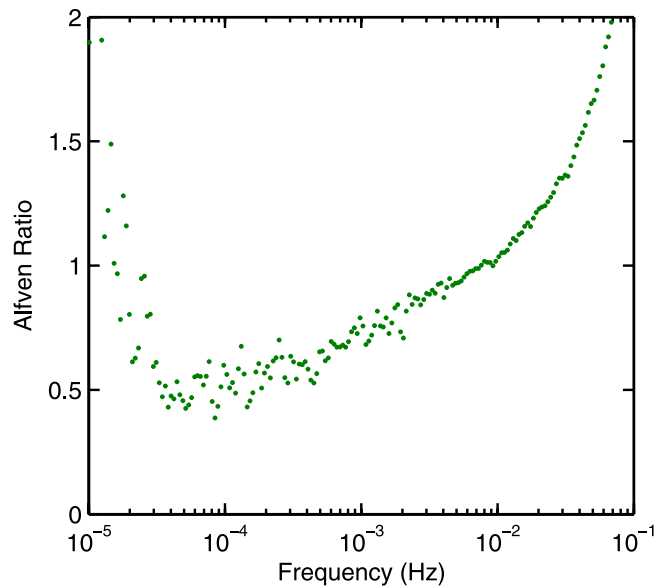
Figure 7. Dimensionless Alfvén ratio, the ratio of kinetic to magnetic energy spectra in Figure 6 as explained in the text. The sharp rise in the Alfvén ratio beyond approximately 2×10^{-2} Hz is not a real effect but is caused by aliasing in the velocity spectrum.

spectral estimation techniques does not appear to have been documented until now. For completeness, the spectral exponents for the components V_x, V_y, and V_z in the subinterval $1 \times 10^{-3} \leq f \leq 1 \times 10^{-2}$ Hz are found to be -1.50, -1.49, and -1.51, respectively. The spectral exponents for

The Alfvén ratio increases from approximately 0.5 to 1.0 between 10^{-4} and 10^{-2} Hz, an increase by a factor of two. These estimates of the Alfvén ratio are consistent with previous studies that indicate a slightly increasing Alfvén ratio with values ranging between 0.4 and 1 in the inertial range of the turbulence and for frequencies less than approximately 5×10^{-3} Hz [*Matthaeus and Goldstein*, 1982; *Roberts et al.*, 1987; *Marsch and Tu*, 1990; *Roberts et al.*, 1990; *B. E. Goldstein et al.*, 1995]. The results in Figure 7 are also in agreement with those of *Salem* [2000] in the range from 10^{-4} to 10^{-2} Hz.

6. Fast Versus Slow Wind

[30]   To investigate the differences in the spectral exponents for fast and slow solar wind streams, the data for the 54 day interval analyzed in the last section is segmented into fast and slow components as shown in Figure 5. Two time intervals containing fast wind and two time intervals containing slow wind are analyzed. The results show that for the slow wind, the power law exponents for the velocity and magnetic field are near 1.5 and 1.7, respectively, similar to the entire 54 day interval. The fast wind is different, with power law exponents for the magnetic field that are close to 1.6. Further details are provided below.

[31]   The duration of the intervals containing fast wind are 4.89 days for the interval near day 152 and 3.25 days for the interval near day 172 with an average speed for the x-component of 671 and 655 km/s, respectively. The duration of the intervals containing slow wind are 7.14 days for the interval near day 165 and 12.07 days for the interval near day 190 with an average speed for the x-component of 338 and 332 km/s, respectively. For velocity or magnetic field components possessing an apparent linear trend or having significantly different initial and final values, a line connecting the initial and final values is subtracted from the data before computing the power spectrum. Power spectra were then computed without data tapering in the same way described in section 2. The bandwidth of the lag window is $\Delta f = 0.15 \, f$.

[32]   The frequency band used to estimate spectral exponents has a width of one decade and a lower endpoint between 1×10^{-3} and 3×10^{-3} Hz. The errors arising from the linear fits are on the order of two or three percent, but this does not include errors in the spectral estimates themselves which are negligible for the full 54 day interval but less so for the smaller statistical samples considered in this section. Precise error estimates are omitted because the spectral exponents of fast and slow wind are an aside to the main body of the paper.

[33]   For the two intervals containing slow wind the power law exponents found for the velocity spectrum (sum of spectra for the three components) are 1.48 and 1.52, and, for the magnetic field, 1.69 and 1.75. These pertain to the first and second intervals studied, that is, the one near day 165 and the one near day 190, respectively. Thus the values of the power law exponents for the slow wind are close to those found for the entire 54 day interval. For fast wind, the power law exponents found for the velocity spectrum are 1.48 and 1.56, and, for the magnetic field spectrum, 1.56 and 1.61. These refer to the first and second intervals studied, that is, the one near day 152 and the one near

day 172, respectively. Thus for the fast wind the the power law exponent for the velocity spectrum is around 1.5 while the power law exponent for the magnetic spectrum is around 1.6.

[34]   In both fast and slow speed wind the spectral exponents for velocity and magnetic field spectra are different while the magnetic spectrum always has the steeper spectral slope. For the two intervals studied here, the difference between the power law exponents for the magnetic spectrum and the velocity spectrum are, on average, 0.22 for the slow wind and 0.07 for the fast wind. Thus the power law exponents for velocity and magnetic field spectra are closer together in the fast wind. The difference between the spectral exponents of velocity and magnetic field spectra is one way to characterize the different nature of the turbulence in fast and slow streams.

7. Summary and Conclusions

[35]   From the analysis of one 54-day interval of data from the Wind spacecraft it has been shown that the kinetic energy spectrum based on power spectra for the bulk proton velocity in the ecliptic plane at 1 AU near solar minimum has a power law exponent near 3/2 in the inertial range of the turbulence. For this 54-day interval the power law exponent for the velocity spectrum is significantly different than the Kolmogorov value 5/3 that characterizes the magnetic energy spectrum. Because the magnetic energy spectrum decays more rapidly than the kinetic energy spectrum and the Alfvén ratio is on the order of unity in the inertial range, the total energy spectrum (kinetic plus magnetic) decays like the kinetic energy with a frequency dependence $f^{-3/2}$. In addition, because the power law exponents of velocity and magnetic field spectra are different, the Alfvén ratio increases slowly throughout the inertial range indicating that the energy contained in small-scale velocity fluctuations is increasing relative to the energy contained in the magnetic field fluctuations.

[36]   It is important to emphasize that the results of this study do not suggest the kinetic energy spectrum in the solar wind always has a spectral index near 3/2. This result only applies to the one 54-day interval studied here and may be different for other time intervals. Indeed, *Matthaeus and Goldstein* [1982] give an example of solar wind power spectra from Voyager 1 in the ecliptic plane near 1 AU and during the rising phase of solar cycle 21 where both the magnetic and total energy spectra exhibit spectral indices near 5/3. Therefore the results presented here are not believed to be universal.

[37]   One of the shortcomings of the analysis presented here is that the kinetic energy spectra do not take into account the fluctuations in plasma density. The density fluctuations will affect the kinetic energy spectrum and can be included by multiplying the velocity vector by the square root of the density before computing the power spectrum. This is not expected to effect the results significantly but is an important question for future research. Such an analysis will also produce more accurate estimates of the Alfvén ratio. The contribution of alpha particles to the kinetic energy spectrum, omitted from the present work, can also be studied using 3-s 3DP data.

[38] Another topic for future investigation is the determination of spectral exponents for the Elsasser variables. When the equations of magnetohydrodynamics (MHD) are expressed in terms of Elsasser variables the equations become more symmetric and closely resemble the Navier-Stokes equations for nonconducting fluids. Moreover, inner products of the Elsasser variables are conserved quantities in ideal magnetohydrodynamics. Therefore within the context of magnetohydrodynamics these variables are "more natural" from a theoretical point of view than the dependent variables v and B.

References

Goldstein, B. E., E. J. Smith, A. Balogh, T. S. Horbury, M. L. Goldstein, and D. A. Roberts (1995), Properties of magnetohydrodynamic turbulence in the solar wind as observed by Ulysses at high heliographic latitudes, *Geophys. Res. Lett.*, 22, 3393.

Goldstein, M. L., and D. A. Roberts (1999), Magnetohydrodynamic turbulence in the solar wind, *Phys. Plasmas*, 6, 4154.

Goldstein, M. L., D. A. Roberts, and W. A. Matthaeus (1995), Magnetohydrodynamic turbulence in the solar wind, *Annu. Rev. Astron. Astrophys.*, 33, 283.

Leamon, R. J., C. W. Smith, N. F. Ness, W. M. Matthaeus, and H. K. Wong (1998), Observational constraints on the dynamics of the interplanetary magnetic field dissipation range, *J. Geophys. Res.*, 103, 4775.

Lepping, R. P., et al. (1995), The WIND magnetic field investigation, *Space Sci. Rev.*, 71, 207.

Lin, R. P., et al. (1995), A three-dimensional plasma and energetic particle investigation for the Wind spacecraft, *Space Sci. Rev.*, 71, 125.

Mangeney, A., C. Salem, P. L. Veltri, and B. Cecconi (2001), Intermittency in the solar wind turbulence and the Haar wavelet transform, in *Proceedings of the Les Woolliscroft Memorial Conference*, edited by B. Warmbein, *Eur. Space Agency Spec. Publ., ESA-SP-492*, 53.

Marsch, E., and C.-Y. Tu (1990), On the radial evolution of MHD turbulence in the inner heliosphere, *J. Geophys. Res.*, 95, 8211.

Matthaeus, W. H., and M. L. Goldstein (1982), Measurement of the rugged invariants of magnetohydrodynamic turbulence in the solar wind, *J. Geophys. Res.*, 87, 6011.

Percival, D. B., and A. T. Walden (1993), *Spectral Analysis for Physical Applications*, Cambridge Univ. Press, New York.

Podesta, J. J. (2006), Statistical bias in periodograms derived from solar wind time series, *J. Geophys. Res.*, 111, A07103, doi:10.1029/2005JA011233.

Podesta, J. J., and D. A. Roberts (2005), Statistical stationarity of solar wind time series, in *Solar Wind 11*, edited by B. Fleck and T. H. Zurbuchen, *Eur. Space Agency Spec. Publ., ESA-SP-592*, 531.

Roberts, D. A., L. W. Klein, M. L. Goldstein, and W. H. Matthaeus (1987), The nature and evolution of magnetohydrodynamic fluctuations in the solar wind: Voyager observations, *J. Geophys. Res.*, 92, 11,021.

Roberts, D. A., M. L. Goldstein, and L. W. Klein (1990), The amplitudes of interplanetary fluctuations: stream structure, heliocentric distance, and frequency dependence, *J. Geophys. Res.*, 95, 4203.

Salem, C. (2000), Ondes, turbulence et phénomènes dissipatifs dans le vent solaire à partir des observations de la sonde Wind, Ph.D. dissertation, Univ. PARIS 7/Obs. de Paris, Paris, France.

———————————

M. L. Goldstein, J. J. Podesta, and D. A. Roberts, Laboratory for Solar and Space Physics, NASA Goddard Space Flight Center, Code 612.2, Greenbelt, MD 20771, USA. (jpodesta@solar.stanford.edu)